K&C Science Report – Phase 1
Developing Rice Decision Support Tools

William Salas
Applied Geosolutions, LLC
87 Packers Falls Rd
Durham, New Hampshire, USA 03857
Email: wsalas@agsemail.com
Ph: (603) 659-3363, Fax: (603) 659-0419

Collaborators
Nathan Torbick
Applied Geosolutions, LLC
87 Packers Falls Rd
Durham, New Hampshire, USA 03857

Xiangming Xiao
Department of Botany and Microbiology &
Center for Spatial Analysis
University of Oklahoma
Norman, Oklahoma, USA 73019

Changsheng Li
University of New Hampshire
Complex Systems Research Center
Durham, New Hampshire, USA 03857

Cuizhen Wang
Department of Geography
University of Missouri
Columbia, Missouri, USA 65211

Yuan Zhang
College of Environmental & Resources Sciences
Zhejiang University
Hangzhou 310029, China

Jiaguo Qi
Center for Global Change and Earth Observations
Department of Geography
Michigan State University
East Lansing, Michigan, USA 48824

***Abstract*- Primary goals of JAXA's Kyoto and Carbon Initiative are to utilize ALOS PALSAR to enhance agricultural monitoring systems and improve estimates of Greenhouse Gas (GHG) emissions under the "CCC" framework. During Phase 1 of the K&C Initiative, a series of technical objectives were executed to design and apply optimal algorithms to map rice paddies, crop intensity, rice attributes (e.g., biomass), and inundation status. Multi-temporal, multi-mode, and multi-scale (FBS/FBD, AUIG ScanSAR ORT/GRD WB1, K&C GRD Strips) data were used during algorithm development at sites in Poyang Lake, Jiangxi Province and Zhejiang Province, China; Java, Indonesia; and the Sacramento Valley, California, USA. Field-level validation found the fine-beam (FBS, hh, 12.5m) rice paddy- and ScanSAR (hh, 100m) inundation status- PALSAR products to have very high overall accuracies of 95%. These thematic information products derived from PALSAR measurements were used as parameterization into a biogeochemical model to assess GHG emissions and the impacts of different agricultural managements. Biogeochemical simulations showed hydroperiod management to influence methane and GHG emissions by an order of magnitude in terms of metric tons of methane and carbon dioxide equivalence per hectare. The optimal algorithms were applied to regional orthorectified (ORT) ground-range (GRD), HH-mode imagery to create large-area maps of rice in an operational context. These operational PALSAR rice products are being used to understand human environment interactions and improve agricultural monitoring.**

***Index Terms*- ALOS PALSAR, K&C Initiative, rice mapping, agriculture, biogeochemical modelling, wetlands**

I. INTRODUCTION

A. *Overview*

Rice is an important crop globally that influences regional economies and global trade, health and food security, and the Earth system. Rice is the predominant food staple in many regions with more than 400 million tones (milled basis) in production annually with 95% of cultivation in developing regions[1]. Rice land use globally is approximately 13048 million hectares and cultivation utilizes extensive human and natural resources[2]. Due to the important role of rice in the global ecosystem, improved rice monitoring tools are desired by a wide range of decision makers.

In the past decade a number of studies have highlighted the advantages of L-band Synthetic Aperture Radar (SAR) for wetland assessment. The primary advantage of L-band SAR data is its ability to penetrate canopies and its sensitivity to vegetation structure, water content, and biomass independent of weather conditions. The relationship between backscatter and valued ecosystem attributes (i.e., rice biomass) of interest can be modeled over large areas independent of weather making it extremely useful for rice monitoring and resource inventory. L-band rice and wetland applications have included biomass and phenology monitoring, assessing flood dynamics, and differentiating aquatic ecosystems among others.

As part of JAXA's Kyoto and Carbon Initiative (K&CI), Applied Geosolutions is developing a comprehensive Rice Decision Support System to provide end-users information required to make informed decisions. This scientific progress report summarizes progress made by Applied Geosolutions during the JAXA K&CI Phase 1activities during 2006~2008.

II. KYOTO AND CARBON INITIATIVE PHASE 1 FOCI

A. *Relevance to the K&C drivers*

The overarching themes of the JAXA K&CI are guided by the three **C**'s: **C**onventions, **C**arbon and **C**onservation. Under that guiding framework the rice monitoring system provides information products to address issues related to land use patterns and climate change in the context of improving our understanding of human-environment interactions. During Phase 1 the activities and rice products have contributed to:

- Map rice paddies and land use patterns;
- Assess the impacts of rice management decisions on methane and greenhouse gas emissions;
- Improve LULC datasets for scientists;
- Map and model rice growth and rice attributes;
- Monitor crop cycles.

B. *Sites*

Phase 1 applications and algorithm development were performed at three primary sites. Site one (fig. 1) is the Poyang Lake region in Jiangxi Province, China (centered ~116.10E, 28.50N) and an area in Zhejiang Province, China. Poyang Lake is the largest freshwater body in China and has significant ecological value with rare migratory waterfowl and extensive wetlands making the Ramsar classified-site an international recognized ecosystem of value. These factors have led to the Poyang Lake region being an international field-site with many integrated studies.

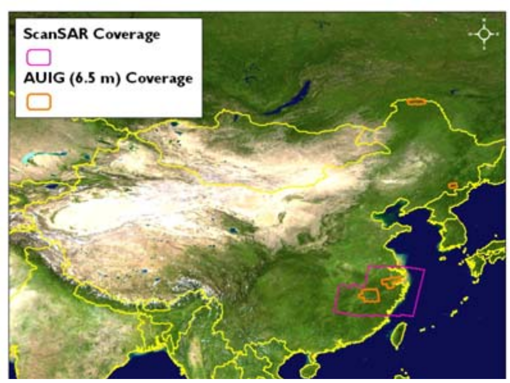

Figure 1. Algorithm development site 1 is the Poyang Lake region in Jiangxi Province, China. Image polygons highlight the development regions where PALSAR algorithms were created and evaluated using FBS and ScanSAR WB1 ORT/GRD data from AUIG.

The Poyang Lake (fig. 2) region has extremely dynamic hydrology with periodic flooding from central Yangtze River basin fluctuations and widespread levee systems altering flows. Extensive and scattered rice paddies are dispersed south of the lake within a patchy landscape of paddies, aquaculture, urban centers, villages, and natural covers. Over the past few decades of economic growth in China, many of the wetland areas are being converted for rice agriculture[3]. The site is subtropical with average annual precipitation and temperature at 170cm and 17degrees C, respectively.

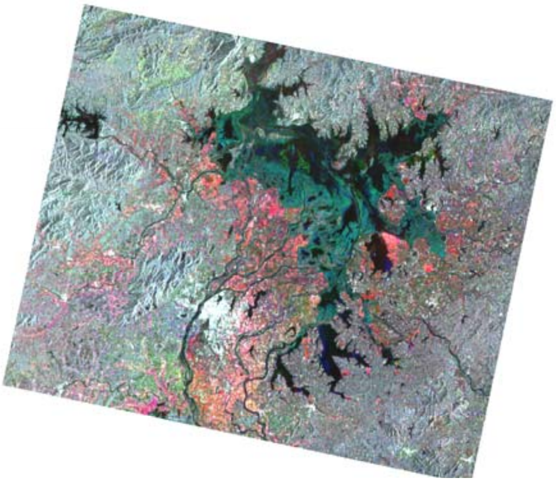

Figure 2. The Poyang Lake region, Jiangxi Province, China was a primary model development site during Phase 1. Multi-temporal AUIG ScanSAR ORT/GRD (Red: DOY241, Green: DOY149, Blue: DOY103) WB1 (HH: 100m). Bright red displays rice paddies and bright white urban land uses.

Site 2. Site two is a large, commercially important rice growing region located in the northern Sacramento Valley, California, USA (centered ~121.825W, 39.20N). Approximately 95% of rice grown in California is grown in this region and it generates nearly half a billion dollars annually to the state's economy. The eight counties in site two that have substantial rice paddy agriculture include: Butte, Colusa, Glenn, Placer, Sacramento, Sutter, Yolo, and Yuba. Other dominant LULC classes in the region include sub/urban, natural vegetation, deciduous fruits and nuts, and field crops. Average temperatures are 45 and 73degrees F in January and July, respectively. Annual precipitation in Sacramento averages 17.2 inches; whereas, annual precipitation in Redding in the northern part of the Sacramento Valley averages 40.9 inches. Intensive irrigation and agricultural management occurs in the area.

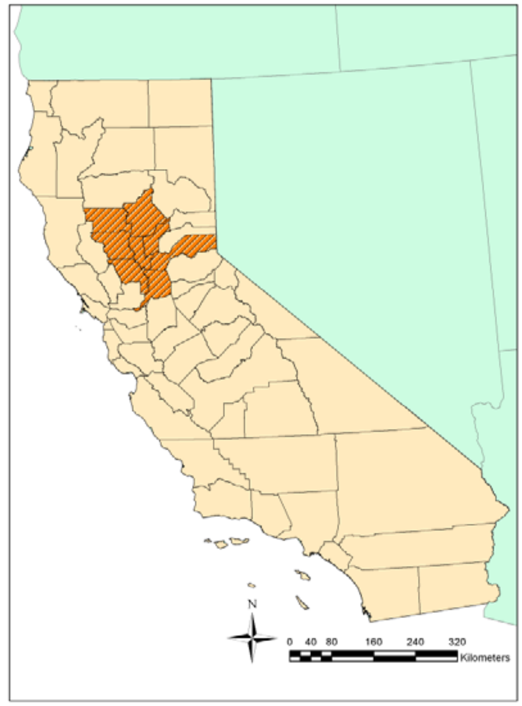

Figure 2. Development and application site 2 was the northern Sacramento Valley, California, USA. PALSAR rice products derived from FBS (HH: 12.5m) and ScanSAR WB1 ORT/GRD (HH: 100m) data were used to parameterize a biogeochemical model to assess rice management decisions and impacts on greenhouse gas emissions.

Site 3. Site three is the island of Java, Indonesia (centered ~110W, 7S). The tropical island is approximately 132,000km^2 and is one of the world's leading rice producers with more than 50 million tones annually and 13 million hectares cultivated. The region has dramatic topographic changes and rice is grown at a variety of altitudes with a range of continuous crop cycles. The majority of rice paddies in Java are under some mechanism of irrigation control with only 10% considered rainfed lowlands. Large urban populations and coastal communities tend to cultivate *indica* subspecies. Paddies range from large-area commercial farms to terraced rice and isolated communities in the highlands creating a challenging rice mapping environments in this tropical climate.

Figure 3. Development site 3 is Java, Indonesia. The algorithms were developing using FBS and WB1 imagery and are being scaled up to the Pan Asian region using K&C strip imagery.

C. Approach

A series of technical benchmarks were evaluated in order to identify optimal algorithms for rice monitoring. Costume python scripts automatically retrieve data from JAXA ftp servers. Pre-processing scripts perform multiple tasks that include: file format conversions (create geotiffs, Digital Number images, backscatter images), re-project (Albers Conic Equal Area for K&C strips and UTM for AUIG imagery), geometric viewing calculations, and file organization (fig.4). The best available Digital Elevation Model was used for each development site. International sites used 90m Shuttle Radar Topography Mission (SRTM)[4] data while USA sites used 30m SRTM data for local incident corrections.

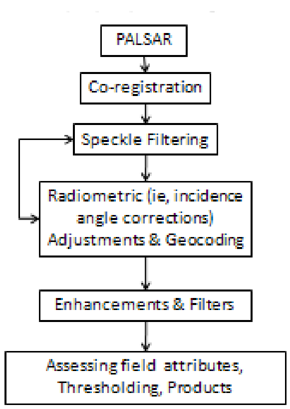

Figure 4. Secondary pre-processing steps apply a linear, multi-temporal speckling filter and perform radiometric enhancements and terrain geocoding adjustments to correct for local incident angles and viewing geometry effects using the best available Digital Elevation Model. Once secondary pre-processing is complete PALSAR imagery is ingested into the product generation stream.

Technical objectives were designed to identify optimal algorithms to monitor rice using a complementing suite of PALSAR resolutions. Initially algorithm development used AUIG fine-beam, hh-mode, 12.5m spatial resolution PALSAR. Once the algorithms were designed they were scaled up and applied to AUIG ScanSAR ORD/GRD WB1 and K&C strip imagery. The primary objectives completed during Phase 1 were to develop algorithms to:

- map rice paddies
- map rice cropping systems
- map inundations status
- map biophysical characteristics

Once secondary pre-processing (fig. 4) was complete the fully pre-processed PALSAR imagery was ingested into the second processing stream. A simple decision-tree framework based on thresholding FBS values was first used to identify rice paddies by capturing the characteristics of flooded areas and dynamic range representing rice phenology and harvest. Next, segmentation procedures are performed to create individual classified polygons or rice paddies. For each rice paddy, informative products were generated based on PALSAR K&C Strip measurements or AUIG ScanSAR ORT/GRD WB1 data. Multi-temporal PALSAR is used to identify crop cycles, flood status, and phenology/biomass changes for each rice paddy. Empirical rice growth models and various post processing tools are used to refine those products (fig. 5).

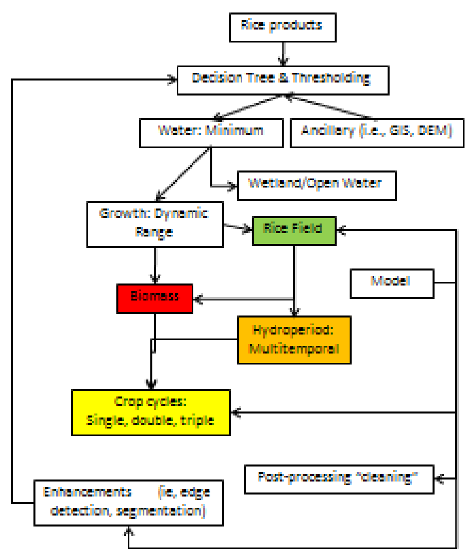

Figure 5.The product generation stream ingests fully pre-processed PALSAR imagery to provide spatially-explicit rice information products including biomass, crop cycles, and hydroperiod.

The generated products for site 2 were used to meet climate change assessment objectives and K&I "**CCC**" overarching goals. The primary objectives under the climate change assessment context during Phase 1 were to:

- Parameterize models with PALSAR rice products
- Simulate impacts of rice managements
- Assess impacts of rice managements on GHG emissions and climate change

D. Satellite data

A range of PALSAR imagery was utilized during Phase 1. FBS and ScanSAR WB1 products (level 1.5) were used at sites 1 and 2. K&C strip ORD/GRD data were utilized at site 3 for operational mapping at continental scales. Spatial resolutions ranged from 6.25m to 100m pixel spacing. Modes included single, dual, and quad pole. Processed levels ranged from JAXA level 1.0-1.5 file formats with automated scripts transforming data into DN and backscatter values (equation 1) and re-projecting to desired coordinate systems. Multiple temporal periods for each site were obtained to capture key rice phenological attributes.

- $\sigma 0 = 10 * \log10(DN2) + CF$ (eq. 1)

Table 1. AUIG PALSAR imagery used during Phase 1. Orbits include both descending and ascending, product levels 1.1 & 1.5, with ranging incidence angles.

Mode	Res (m)	Temporal	Scenes
FBS	6.25	multi (2006-2008)	58
FBD	12.50	multi (2006-2008)	55
WB	100.00	multi (2006-2008)	57

Local incident angle corrections utilized the best available Digital Elevation Model (DEM) for each development site. International sites used 90m Shuttle Radar Topography Mission (SRTM)[4] data while USA sites used 30m SRTM data.

For site 3 operational monitoring K&C strip data was utilized (Table 2). As part of JAXA's K&CI, a PALSAR acquisition strategy has been developed with a goal of having spatially and temporally consistent data at continental scales with adequate revisit frequency and timing to enable the development of continental-scale products. The wetlands science team led the development of the PALSAR acquisition strategy that includes ScanSAR data acquisitions every 46 days for regional mapping and characterization of wetlands and paddy rice in Southeast Asia. Adjacent acquisitions overlap 50%, so effectively there are 2 acquisitions every 46 days continuously from October 2006 to September 2009.

E. Field campaign & reference data

An accuracy assessment was carried out and completed during Phase 1 at Site 2. FBS (HH mode, 12.5m) rice paddy classifications and ScanSAR WB1 (HH mode, 100m) inundation status products were assessed for overall accuracy and misclassification patterns. A series of error matrices were constructed using the field-level data and high resolution color photography as reference. For the FBS HH rice products, orthorectified National Agriculture Imagery Program (NAIP) mosaics were utilized as ground control reference. NAIP data collection occurred near Day of Year (DOY) 215 and 253 which is during the rice growing season at site 2. These true-color, 1-meter, digital photos are available through the United States Department of Agriculture (USDA) Geospatial Data Gateway. Data are compressed in MrSid format with a horizontal accuracy of less than 3 meters. Mosaics are tiled using a 3.75' x 3.75' quarter quads formatted to the UTM projection system using North American Datum 1983 (NAD83). Bounding coordinates covered the entire spatial domain that PALSAR imagery covered. Additional metadata are available via the USDA data gateway.

For the FBS HH rice products a stratified random sampling scheme was utilized to insure statistical sampling rigor following well-established accuracy protocol. The validation scheme identified the maximum classified proportion to generate a specified sample number (475). A stratified random distribution with 250 rice points separated with a minimum distance of 300m was applied within the PALSAR rice product. A second suite of stratified random points were distributed among non-rice classes based on the ancillary LULC data from the Department of Water Resources (DWR) in California. Together these assessment data points provided 475 unique, statistically rigorous validation points. The accuracy points were checked using a variety of techniques. All points were compared against DWR LULC data and verified against the NAIP imagery.

For the ScanSAR inundation status products a near-simultaneous field campaign was performed to assess the accuracy of the flood products at site 2. The overpass date was January 20, 2009. ScanSAR image scene centers were 40.464N x 120.379W and 37.991N x 120.977W. From the binary FBS rice maps two large clusters were chosen as focus areas for the winter flood assessment. The clusters were approximately 50km north of the City of Sacramento and 25km west of the City of Oroville. Ground truth data were collected using a GPS-enabled camera at approximately 1000m equal intervals following the road network. "Drive-by" transects were carried out and points were systematically collected within the two pre-selected clusters. GPS photos were collected perpendicular to the road direction using the stratified approach. A total of 130 points were collected for the second portion of the rice product assessment.

Table 2. PALSAR K&C Strip imagery used during Phase 1.

AGS K&C PALSAR Archive (As of January 1, 2009)	Count	Size (GB)
Total Images	345	125
Total Processed Images (ORT Only)	254	119
By Region (China/S. Asia/Indonesia)	36/198/50	15/93/8
Unprocessed Images (SLT/GRD)	44/17	5/1
Modes Available (WB1/FBD/FBS)	285/52/8	119/5/1

F. Biogeochemical modelling

The process-oriented DeNitrification and DeComposition (DNDC) model[5,6,7] was originally developed to simulate the effects of major farming practices (e.g., crop rotation, tillage, fertilization, manure amendment, irrigation, flooding, weeding, grass cutting and grazing) and climate change (temperature and precipitation) on C and N cycles in various ecosystems. By tracking rice biomass production and decomposition rates, DNDC also simulates long-term soil organic carbon (SOC) dynamics, predicts CH_4 and N_2O emissions by tracking the reaction kinetics of nitrification, denitrification and fermentation across climatic zones, soil types, and management regimes[8]. PALSAR rice products were used as model parameterization for site 2 simulations that were completed during Phase 1.

Further, parameterization used the State Soil Geographic (STATSGO) database, which is a digital soil association map developed by the National Cooperative Soil Survey and distributed by the Natural Resources Conservation Service (formerly Soil Conservation Service) of the U.S. Department of Agriculture. It consists of a broad based inventory of soils and nonsoil areas that occur in a repeatable pattern on the landscape and that can be cartographically shown at the scale mapped. Climate data used DAYMET weather data which is a model that generates daily surfaces of temperature, precipitation, humidity, and radiation over large regions of complex terrain.

III. Results and Summary

Algorithm development has been completed during Phase 1. Figures 4 and 5 illustrates the primary image processing steps and PALSAR products generated from the rice monitoring system. To streamline reporting results are summarized by project focus and region.

A. Assessing impacts of rice managements

1. Mapping rice in the Sacramento Valley, USA

A minimum threshold identifies water within a given pixel (fig 6). Water at this stage can be a flooded rice paddy, a natural water body, or a manmade irrigation feature. A branch in the decision tree then applies a maximum or range threshold based off either empirical data or image statistics. This process results in a classification product delineating rice fields according to the rules and data used in the decision tree (fig. 7). A semi-automated data cleansing process enhances data products based on user defined rules. For example, a spatial analysis process eliminates single, isolated pixels to streamline data products.

Figure 6. Early rice paddy flood season (left) seen as dark color and full rice maturation (right) seen as light purple displayed in R:G:B (HH:HV:Difference) from PALSAR FBS/D. A decision-tree thresholding and segmentation approach identify rice paddies across the landscape using flood- and rice growth-backscatter response.

Table 3. Study area *2* inundation status monitoring Approximately half of paddies (47% or 74,292 hectares) were flooded during **December** and 75% of rice paddies were flooded during at least one winter time period.

Hydroperiod	Area (hectares)	Percent
No Winter Flood	37866	24.4
Dec Flood	**74292**	**47.8**
Mar Flood	590	0.4
Dec & Mar Flood	11176	7.2
Apr Flood	8952	5.8
Dec & Apr Flood	17341	11.2
Mar & Apr Flood	159	0.1
Dec, Mar, Apr Flood	5083	3.3

PALSAR-derived rice maps identified nearly 75,000 hectares of rice paddies undergoing cultivation during the temporal FBS overpasses in 2007. Figure 7 displays rice paddies and associated flood regimes near the Biggs Experimental Agricultural Station in the northern Sacramento Valley, California, USA. ScanSAR WB1 imagery with regional coverage twice every 46 days was used to identify inundation status for each rice paddy. Approximately half of all rice paddies in the Sacramento Valley were flooded during a portion of the month of December. During Phase 1 image dates used were 12/5/2006, 3/7/2007, and 4/17/2007 to characterize a typical winter cycle. Approximately half of paddies (47% or 74,292 hectares) were flooded during December and 75% of rice paddies were flooded during at least one winter time period (table 3, fig 8).

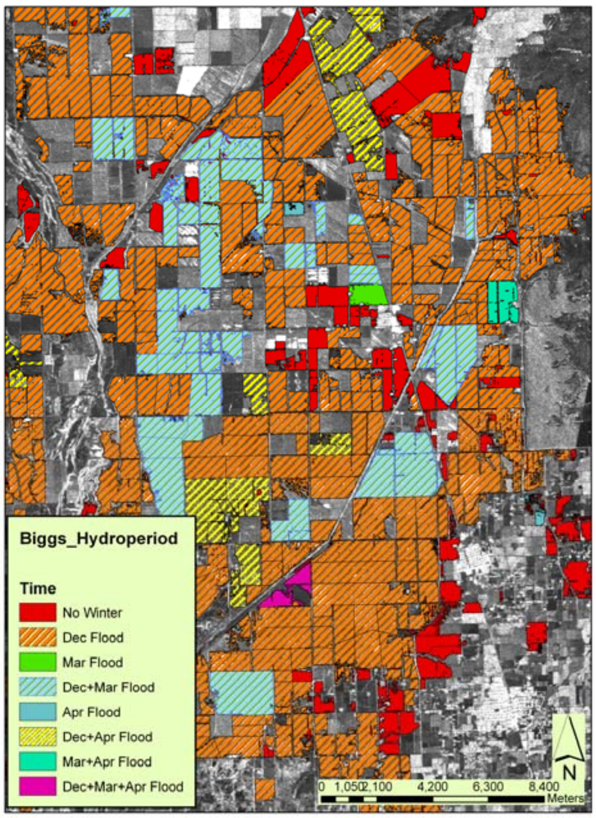

Figure 7. Mapping rice paddies and rice paddy hydroperiod with FBS (HH: 12.5m) and ScanSAR WB1 (HH:100m), respectively. Approximately 75,000 hectares of rice paddies were cultivated in the rice growing season of 2007 in the Sacramento Valley, California, USA. Of these, approximately half (47%) were identified as flooded during December.

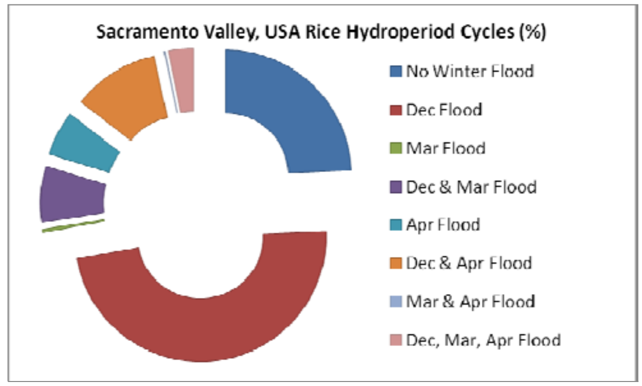

Figure 8. Study area *2* (Sacramento Valley, California, USA) inundation status monitoring with ScanSAR imagery with regional coverage twice every 46 days. Approximately half of paddies (47% or 74,292 hectares) were flooded during December and 75% of rice paddies were flooded during at least one winter time period.

2. *Accuracy of Biggs, USA rice products*

A field-campaign and ancillary reference information found the FBS rice paddy products to possess very high overall accuracy (fig 9). The rice paddy map classification had an overall accuracy of 96% (449 / 469 = 0.9573). Approximately 20 points were interpreted as misclassifications giving an overall omission error of 0.0426. Kappa statistics had a khat value of 0.912609 with a variance and z-score value of 0.00036530 and 47.748, respectively with a p-value significance of <0.00001.

Fieldwork was performed to assess the accuracy of the winter flood products for characterizing inundation status. Two ScanSAR mode scenes were pre-processed and merged to complete coverage over the Sacramento Valley, USA. The overpass date was January 20, 2009. The clusters were approximately 50km north of Sacramento and 25km west of Oroville. Ground truth data was collected using a GPS-camera at approximately equal intervals. Road transects were carried out and points were systematically collected. GPS-photos were collected to perpendicular to the road every using the major routes bisecting the two clusters. A total of 130 points were collected. Interpretation of the ground truth photos resulted in an overall accuracy of 96% (124/129). One point was thrown out due to error.

Figure 9. Two GPS-enabled camera ground truth points at Site 2 showing correct classifications of flooded rice paddies.

The misclassified points were distributed among five categories of errors (fig 10). The majority of these errors were related to temporal challenges. This means that the rules used in the decision tree classifier to define the rice paddies eliminated a potential rice field due to shifts in flood cycles, harvest date, and/or overpass timing. Three errors were related to spatial problems where a point fell just outside a rice polygon or classified rice pixel. Three were related to confusion with dynamic wetland areas.

- Temporal=12
- Spatial=3
- Riparian=3
- Grain=1
- Unknown=1

Figure 10. Ground-truth points from the Biggs, California, USA winter flood assessment found overall accuracy of 95%. ScanSAR imagery was classified into a binary map of water and nonwater pixels to characterize rice paddy inundation. Point 2 illustrates a misclassification caused by slight flooding from accumulated rain fall and saturated soil at the location.

The accurate rice products in this region then served as parameterization for the biogeochemical simulations using the DNDC model. Figure 11 illustrates simulations using the PALSAR-derived parameterizations (ie, inundation status and rice paddy). Results found that flooding regime decisions significantly impacts methane and greenhouse gas emissions.

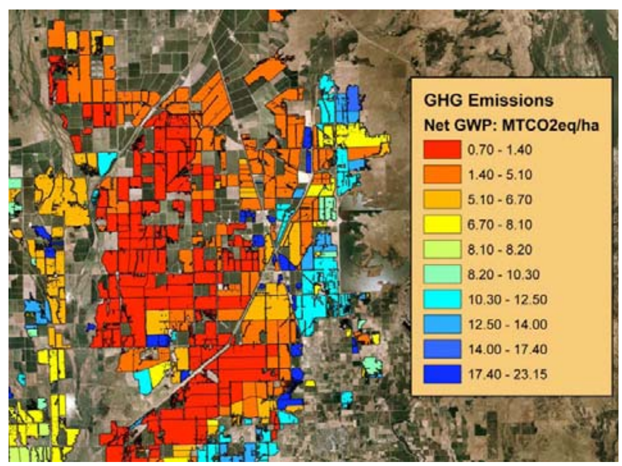

Figure 11. DNDC simulations uses PALSAR-derived rice information. Simulations found that flooding cycle decisions can substantially impact methane and GHG emissions.

B. Mapping paddy rice in China

The PALSAR backscatter coefficient (σ°) images in different dates were stacked into a three-layer composite image (fig. 12). After upland hardwoods were masked out, the non-forest composite image was put in a Support Vector Machine (SVM) algorithm for a five-class thematic map was produced.

Waterbodies were easily identified with clear boundaries. The urban area of Fuyang City was clustered in the upper center of the study area. The class map also demonstrated urbanization and intensified human settlement in lowland plains.

It was shown that rice planting was the major land use type in lowland plains in the study area. Large-area rice cultivation could be easily identified from PALSAR images. However, except for the large flat plains along the Qiantang River in the middle of the study area, paddy rice fields were often small in size and fragmented with other land use surfaces. To demonstrate classification results of these small rice fields, a subset of class map was selected in the north of Xindeng Town, 30km southwest of urban core of Fuyang City. Small rice fields were restricted by local topography and often clustered into narrow and long rice planting area. These areas were smaller and less continuous and resulted in a noisy and scattered pattern in the PALSAR class map. The under-classification of small rice fields was primarily caused by mixed pixels along field edges. These associated borders, however, were assigned rice in survey map because they were associated with rice cropping activities. In the subset, rice planting area detected in the PALSAR-derived map was 4.69×10^6 m^2 while the area in the census map was 5.13×10^6 m^2. Assuming survey map as ground truth, less than 10% of rice area was under-classified.

Two hundred (200) random points in each class were selected and served as validation sites to test the accuracy of the class map. At each validation site, the reference land use type was recorded from survey map. An error matrix of the five classes was built to compare ground-surveyed and image-classified results. The PALSAR class map in this area had an overall accuracy of 80.1% and Kappa statistics of 0.75. Paddy rice reached a user's accuracy of 90% and producer's accuracy of 76%. The relatively large commission error (24%) of rice mapping was primarily a result of misclassifying rice to dryland crop (19 out of 237) or orchard (16 out of 237). It was reasonable because of the similar backscatter amplitudes of these vegetative land use types. A large commission error also occurred where 21 out of 237 paddy rice fields were misclassified as water, a possible effect of open water in flooded rice fields. This may also partially result from land use change between PALSAR image acquisition (2006) and LULC ground survey (2005). For example, some rice fields in 2005 may be abandoned or converted to fish ponds in 2006. Nevertheless, the conditional Kappa value of paddy rice was 0.87, indicating that rice could be mapped at relatively high accuracy with multi-temporal PALSAR images.

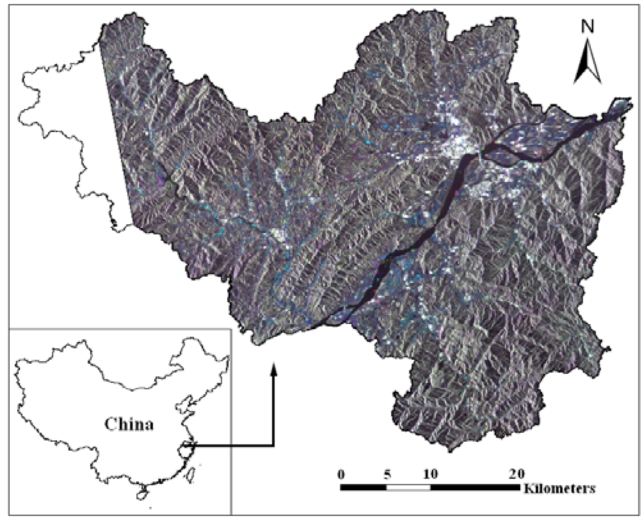

Figure 12. The PALSAR composite image (Jun.18, Aug.3, Sept.18, 2007) in Fuyang City, Zhejiang Province in the southeast China.

With the remarkably high backscatter coefficients, urban structures were classified with the highest user's accuracy of 96.5% and conditional Kappa statistics of 0.95 (fig. 13). Similarly, because of the very low backscatter, water surfaces were also easily classified with a user's accuracy of 80.5%. Some water bodies such as fishing ponds are small and shallow and sometimes covered with water vegetation, which contributed to large omission error (23.7%) of water surfaces. Dryland crops and orchards had the lowest accuracy (conditional Kappa value of 0.63 and 0.58, respectively), because of their backscatter similarity. Since the major objective of this portion of the research was rice mapping, the misclassification of these non-rice land uses was not investigated further.

Comparing with other SAR sensors, PALSAR has a great advantage in rice mapping[9]. Firstly, PALSAR has multi-mode imaging capabilities to acquire SAR imagery at varying resolutions and swaths, which provides flexible applications to fulfill tasks at various scale, extent and accuracies as well as costs. For example, the PALSAR images at FBS mode (6.25m pixel size) applied in this study could extract small and fragmented rice planting area, while the ScanSAR-mode images (100-m pixel size) could be more efficient in regional rice mapping. Among all SAR systems that are currently operating or operated in past years, only Radarsat-1/2 have the same multi-mode feature.

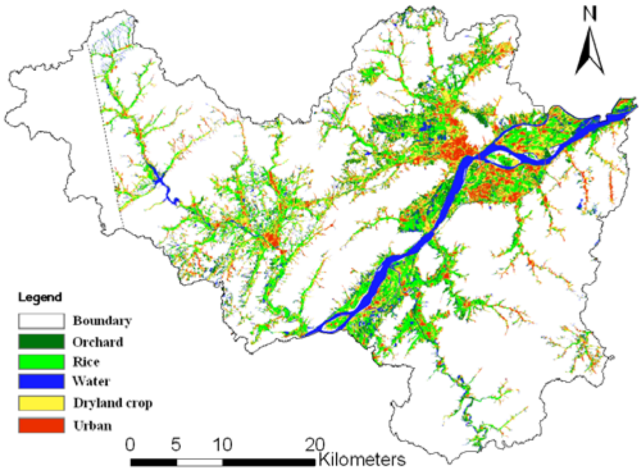

Figure 13. The class map derived from multi-temporal PALSAR images. The upland forest is masked out[9].

Secondly, except for a polarimetric sensor onboard the newly launched Radarsat-2 (in December 2007), PALSAR is the only sensor that could acquire imagery in multiple polarizations (HH, HV, and VV).

Thirdly, as a successor of JERS-1 SAR, PALSAR is the only sensor that operates in relatively low frequency (L-band). L-band signals could penetrate deeper into rice canopy and therefore, may contain more information about total rice biomass than C-band signals of other systems. It has been demonstrated in past studies that different rice biophysical parameters were sensitive to backscatter in different polarizations and frequencies[10]. This information could be applied in radiative transfer models to quantify rice biophysical properties such as leaf area index and fresh biomass, which is closely related to rice production.

C. Modeling rice attributes

This portion of the study examined L-band scattering properties of paddy rice with multitemporal PALSAR imagery, field measurements (fig 14), and a radiative transfer model[11]. Leaf volume scattering and leaf-ground double bounce in L-band were found the major scattering components that increased with plant height and leaf mass amount. In tillering and heading stages, HH backscatter was more sensitive to rice's structural variation while VV backscatter remained almost constant along rice growth cycle (fig. 15).

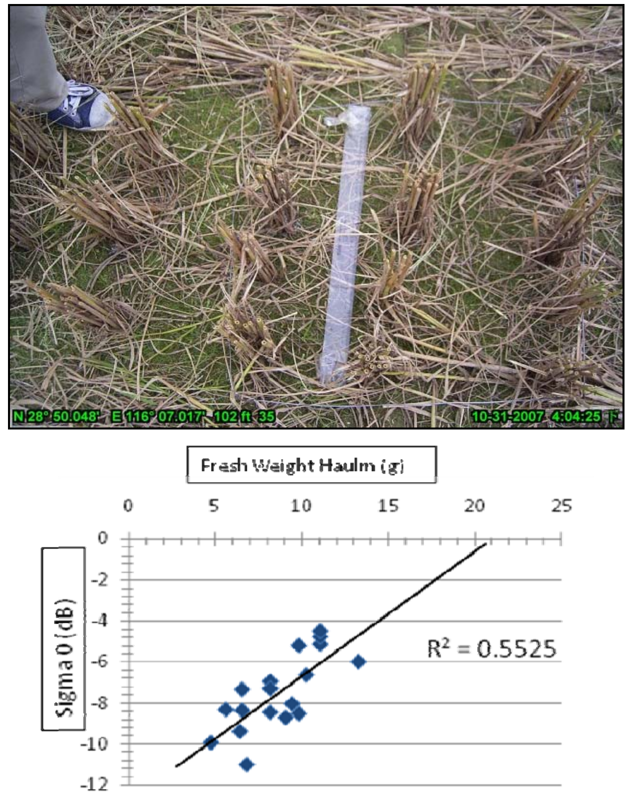

Figure 14. Top) Poyang Lake field site measuring valued rice ecosystem attribute: haulm weight, plant height, water depth, paddy density, and planting patterns. Measurements were used to develop model parameters to forecast growth cycles and PALSAR backscatter responses. Bottom) Fresh haulm weight was quantified and converted into density-adjusted biomass. These measurements were correlated against PALSAR FBS HH 12.5m to identify optimal algorithms and map paddy attributes.

These results show that multi-temporal L-HH backscatter may be more useful in rice biophysical mapping and modeling studies. HV backscatter was affected by multiple interactions between radar signals and rice canopies and cannot be accurately simulated via 1st-order canopy scattering model.

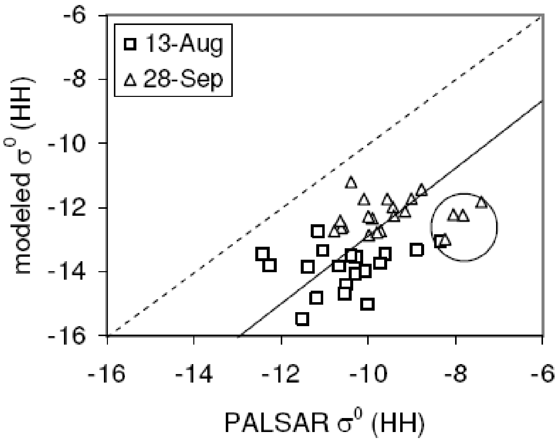

Figure 15. The scatterplot of modeled and PALSAR observed HH backscatter in three rice growth stages[11].

D. Ongoing efforts

During the extension period assessments will be performed on products for Java and Poyang Lake. Due to data delays the Pan Asian maps are now underway as well. Extensive field campaigns with partner projects will provide additional accuracy information.

ACKNOWLEDGEMENTS

This work has been undertaken within the framework of the JAXA Kyoto & Carbon Initiative. ALOS PALSAR data have been provided by JAXA EORC. Additionally support has been provided by JAXA, NASA LCLUC (#NNX08AL16G) and the National Institutes of Health (NIH).

REFERENCES

[1]International Rice Research Institute. World Rice Statistics. Statistical Database. http://irri.org.

[2]Tpriyama, K., Heong, K., Hardy, B. editors, 2005. Rice is life: scientific perspectives for the 21st century. Proceedings of the World Rice Research Conference, Tokyo, Japan. International Rice Research Institute.

[3]Jiang, L., Bergeb, K., Brown, D., Zhao, T., Tian, Q., Qi, S. 2008. Land-cover change and vulnerability to flooding near Poyang Lake, Jiangxi Province, China. *Photogrammetric Engineering & Remote Sensing*, 74, 1-12.

[4]Jarvis A., H.I. Reuter, A. Nelson, E. Guevara. 2008. Hole-filled seamless SRTM data V4, International Centre for Tropical Agriculture (CIAT); http://srtm.csi.cgiar.org.

[5]Li, C., S. Frolking, and T.A. Frolking, 1992a, A model of nitrous oxide evolution from soil driven by rainfall events: 1. Model structure and sensitivity, *Journal of Geophysical Research*, 97:9759-9776.

[6]Li, C., V. Narayanan, and R. Harriss, 1996, Model estimates of nitrous oxide emissions from agricultural lands in the United States, *Global Biogeochemical Cycles* 10:297-306

[7]Li, C., 2000, Modeling trace gas emissions from agricultural ecosystems, *Nutrient Cycling in Agroecosystems* 58:259-276.

[8]Li, C., J Qiu, S. Frolking, X. Xiao, W. Salas, B. Moore III, S. Boles, Y. Huang, and R. Sass, 2002. Reduced methane emissions from large-scale changes in water management in China's rice paddies during 1980-2000, *Geophysical Research Letters*, 29(20), doi:10.1029/2002GL015370, 2002.

[9]Zhang, Y., Wang, C., Wu, J., Qi, J., Salas, W.2009. Mapping Paddy Rice with Multi-temporal ALOS PALSAR Imagery in Southeast China. *International Journal of Remote Sensing.* (accepted/in press).

[10]Le Toan, T., Ribbes, F., Wang, L.F., Nicolas, F., Ding, K.H., Kong, J.A., Fujita, M. and Kurosu, T., 1997, Rice crop mapping and monitoring using ERS-1 data based on experiment and modeling results. *IEEE Transactions on Geoscience and Remote Sensing*, **35**, 41-56.

[11]Wang, C., Wu, J., Zhang, Y., Pan, G., Qi, J., Salas, W. 2009. Characterizing L-band scattering of paddy rice in southeast China with radiative transfer model and multi-temporal ALOS/PALSAR imagery. *IEEE Transactions on Geoscience and Remote Sensing.* (accepted/in press).

JAXA K&CI PI.

William A. Salas is President and Chief Scientist of Applied Geosolutions, LLC in New Hampshire, USA. Dr. Salas has degrees in mathematics, forestry, and natural resources from the Universities of Vermont and New Hampshire, respectively. He formed AGS in the year 2000 to promote, support and provide scientifically sound cutting-edge geo-spatial technologies, biogeochemical modeling applications, and integrated spatial information services. AGS works with private companies, universities, governments, NGOs, and federal agencies.

Collaborators.

Nathan Torbick is a Research Scientist at Applied Geosolutions In New Hampshire, USA. Dr. Torbick joined AGS after completely his graduate work at the Center for Global Change and Earth Observation at Michigan State University. His research foci are human-environment interactions, aquatic ecosystem assessment, and geospatial technologies.

Xiangming Xiao earned a Bachelor's degree in Biology from Xiamen University, China in 1982, and a Master's degree in Plant Ecology from Institute of Botany, Chinese Academy of Science and University of Science and Technology, China in 1987, and a UNEP/UNESCO's Diploma of Environmental Management and Protection from University of Technology, Dresden, Germany in 1988, and a Ph.D degree in Ecosystem Science from Colorado State University in 1994. Dr. Xiao recently began a new position at the University of Oklahoma after working at the Complex Systems Research Center at the University of New Hampshire. His research interests span a wide range of biological science, geo-science and health science, including climate change, land use and land cover change, global carbon cycle, remote sensing, and epidemiology and ecology of infectious diseases.

Changsheng Li received his Bachelor's degree in Geochemistry from University of Science and Technology of China in 1964, Master's degree in Environmental Chemistry from Chinese Academy of Sciences in 1981, and Ph.D. degree in Biogeochemistry from Chinese Academy of Sciences and University of Wisconsin in 1985. He has been devoted to biogeochemical and environmental studies since. In 1992 he moved to the University of New Hampshire where he is now Research Professor in the Complex Systems Research Center within the Institute for the Study of Earth, Oceans, and Space. His academic interest is to explore the theories and methodologies which can be used for revealing relationship between humankind and their environment. Dr. Li has been focusing his study on biogeochemical cycling of chemical elements, especially its numerical expression in time and space.

Chuizhen Wang is an Assistant Professor at the University of Missouri in the Department of Geography. Chuizhen joined UM after completing her PhD at Michigan State. Dr. Wang's primary research areas are bio-environmental remote sensing, GIS and spatial analysis. Particular interests are in biodiversity, biophysical retrieval, ecosystem and environmental mapping. Her past research experience includes Land Use/Land Cover mapping, canopy radiative transfer modeling, and quantitative biophysical estimation with optical and microwave remotely sensed data.

Zhang Yuan received the B.S. degree from Liaoning Normal University, China, in 1998, and the M.A. degrees in Dept. of Forestry, Sheyang Agricultural University, China, in 2003. He is currently a Ph.D candidate in the Institute of Agricultural Remote Sensing and Information Technology Applications, Zhejiang University, China. His research interests are in biophysical and environmental remote sensing and ecosystem simulation.

Jiaguo Qi is the Director of the Center for Global Change and Earth Observation at Michigan State University. His research is focused on using Earth observations for understanding the coupling of natural and human systems and global change research. He uses a variety of geospatial techniques to better understand the responses/feedbacks of the two coupled processes.